Bulletin of Mathematical Biology (2021) 83:111
https://doi.org/10.1007/s11538-021-00945-w

Society for Mathematical Biology

ORIGINAL ARTICLE

A Zika Endemic Model for the Contribution of Multiple Transmission Routes

Xiaoyan Yuan[1] · Yijun Lou[2] · Daihai He[2] · Jinliang Wang[3] · Daozhou Gao[1]

Received: 11 May 2021 / Accepted: 15 September 2021

Abstract
Zika virus disease is a viral disease primarily transmitted to humans through the bite of infected female mosquitoes. Recent evidence indicates that the virus can also be sexually transmitted in hosts and vertically transmitted in vectors. In this paper, we propose a Zika model with three transmission routes, that is, vector-borne transmission between humans and mosquitoes, sexual transmission within humans and vertical transmission within mosquitoes. The basic reproduction number $\mathcal{R}_0$ is computed and shown to be a sharp threshold quantity. Namely, the disease-free equilibrium is globally asymptotically stable as $\mathcal{R}_0 \leq 1$, whereas there exists a unique endemic equilibrium which is globally asymptotically stable as $\mathcal{R}_0 > 1$. The relative contributions of each transmission route on the reproduction number, and the short- and long-term host infections are analyzed. Numerical simulations confirm that vectorial transmission contributes the most to the initial and subsequent transmission. The role of sexual transmission in the early phase of a Zika outbreak is greater than the long term, while vertical transmission is the opposite. Reducing mosquito bites is the most effective measure in lowering the risk of Zika virus infection.

Keywords Zika virus disease · Sexual transmission · Vertical transmission · Basic reproduction number · Global stability · Relative contribution

Mathematics Subject Classification 37N25 · 34D20 · 92D30

✉ Daozhou Gao
dzgao@shnu.edu.cn

1 Mathematics and Science College, Shanghai Normal University, Shanghai, China

2 Department of Applied Mathematics, The Hong Kong Polytechnic University, Hung Hom, Kowloon, Hong Kong, China

3 School of Mathematical Science, Heilongjiang University, Harbin, China

Published online: 28 September 2021

1 Introduction

Zika virus disease (ZVD), also called Zika fever or simply Zika, is a mosquito-borne disease caused by Zika virus (ZIKV), which belongs to the genus *Flavivirus* from the family *Flaviviridae*. The virus is mainly transmitted to humans by the bites of infected *Aedes* mosquitoes, including *Aedes aegypti* and *Aedes albopictus*. About 20% exposed humans develop symptoms after the intrinsic incubation period of 3–14 days. Common symptoms of Zika include fever, skin rashes, conjunctivitis, and headache (Duffy et al. 2009). Women infected by Zika virus during pregnancy may give birth to newborn babies with microcephaly and other birth defects (Mlakar et al. 2016; Rasmussen et al. 2016). Zika virus infection is also associated with the increasing incidence of some other neurological disorders including Guillain–Barré syndrome (GBS), neuropathy and myelitis (Pan American Health Organization 2016; Parra et al. 2016; World Health Organization 2021). Moreover, the phenomenon of antibody-dependent enhancement may or may not occur in ZIKV infections with prior exposure to dengue virus (Sariol et al. 2018). To date, there is still no licensed vaccine or approved treatment against the virus.

Zika virus was first isolated from the serum of a rhesus monkey trapped in the canopy of the Zika forest in Uganda in 1947, and from the *Aedes africanus* mosquito in the same forest one year later (Dick et al. 1952). It was subsequently discovered in humans from Uganda and Tanzania in 1952 (MacNamara 1954). For decades, Zika virus expanded its geographical distribution from Africa to equatorial Asia, including India, Indonesia, Malaysia and Pakistan, where only sporadic human cases were reported (World Health Organization 2016b). The first recorded Zika virus outbreak occurred on Yap Island, Federated States of Micronesia in 2007 (Duffy et al. 2009). In October 2013, the first large-scale ZIKV outbreaks happened in French Polynesia and subsequently in three other groups of Pacific islands (Musso et al. 2014). Autochthonous cases of Zika virus infection were detected in Brazil in March 2015, and the virus swiftly spread to many other countries in South and Central America and the Caribbean (World Health Organization 2017). On February 1, 2016, the World Health Organization (WHO) declared the Zika outbreak a Public Health Emergency of International Concern (World Health Organization 2016a). An estimated 440,000–1,300,000 Zika cases occurred in Brazil during 2015 (Heukelbach et al. 2016). The virus is still circulating in Brazil and other countries and constitutes a major public health threat.

Besides the mosquito-borne transmission pathway (mosquitoes feed on hosts), Zika virus can also be transmitted through heterosexual or homosexual contact (Moreira et al. 2017; Polen et al. 2018). The potential for sexual transmission of ZIKV was initially discovered by Foy et al. (2011). During the 2015–2016 Zika virus epidemic, the first sexually transmitted Zika case was diagnosed in Dallas County in the USA on February 2, 2016 (DCHHS 2016). Later on, more cases via sexual transmission were documented in the USA and other countries such as Argentina, Canada, Chile, France, Germany, Italy, New Zealand, Peru, Portugal and Spain (Moreira et al. 2017). Meanwhile, recent experimental evidences have confirmed that Zika virus can be transmitted vertically from infected female mosquitoes to their offspring. Thangamani et al. (2016) injected ZIKV into female *Aedes aegypti* mosquitoes and tested that six of

1,738 F_1 adult progeny yielded ZIKV, giving a minimum filial infection rate of 1:290. Lai et al. (2020) found that the vertical transmission rates in F_1 *Aedes albopictus* eggs and adults were 2.06% and 1.87%, respectively. In addition, Zika virus is occasionally transmitted through blood transfusion, organ transplantation and laboratory exposure. For pregnant women infected with Zika virus, there is a possibility that they will infect the fetus through perinatal transmission (Besnard et al. 2014).

Since 2015–16 Zika outbreak, mathematical modeling of Zika virus disease has attracted considerable attention (Wiratsudakul et al. 2018). Kucharski et al. (2016) used an SEIR-SEI epidemic model with only vector-borne transmission to analyze the dynamics of ZIKV transmission during the 2013–14 outbreak in French Polynesia. Gao et al. (2016) proposed a mathematical model on ZIKV taking into account both mosquito-borne and sexual transmission routes, and found that sexual transmission contributes little to the basic reproduction number but has the potential to increase the risk of infection and the scale of the epidemic. Their model was analyzed and extended by Bates et al. (2021) through incorporating balanced birth and death rates for humans, and density-dependent birth rate for mosquitoes. Brauer and his collaborators (Brauer et al. 2016; Towers et al. 2016) considered a Zika model similar to that of Kucharski et al. (2016) but adding sexual transmission and fit the model to the daily incidence data of the 2015 ZIKV outbreak in Barranquilla, Colombia. Wang et al. (2017) formulated a Zika model with the consideration of sexual transmission and the release of genetically modified mosquitoes. Baca-Carrasco and Velasco-Hernández (2016) studied the combined effect of heterosexual transmission and migration in the spread of ZIKV. Maxian et al. (2017) developed an age- and sex-structured model including vectorial and male-to-female and male-to-male sexual transmission and revealed that sexual transmission makes a 4.8% contribution to the basic reproduction number. Agusto et al. (2017a) took male-to-female, male-to-male and female-to-male transmission into consideration and showed that risky sexual behavior among males substantially increases the number of Zika infections. Saad-Roy et al. (2018) formulated an age-structured Zika model with vectorial transmission and male-to-female transmission, and they examined the effect of the incidence function for sexual transmission. Tang et al. (2019) developed a coinfection model to investigate the influence of sexual transmission of Zika on the transmission dynamics of dengue and Zika. Agusto et al. (2017b) analyzed a Zika model with human vertical transmission, newborns with microcephaly and asymptomatic infections. A compartmental model with vertical transmission for both humans and mosquitoes was presented by Imran et al. (2021).

In this paper, we aim to study the joint effect of mosquito-borne transmission, sexual transmission and vertical transmission on the spread of Zika virus. The existing work that is closest to our expectation comes from Olawoyin and Kribs (2018) who constructed a deterministic model of Zika virus that incorporates sexual transmission in humans and mosquitoes, vertical transmission in mosquitoes and vector-borne transmission between humans and mosquitoes. Due to the complexity of the model, they only numerically analyzed the potential impact of multiple transmission modes on infection prevention and control. In the next section, we formulate a mathematically tractable model with three transmission routes for Zika virus disease. In Sect. 3, we compute the basic reproduction number, establish the global threshold dynamics and

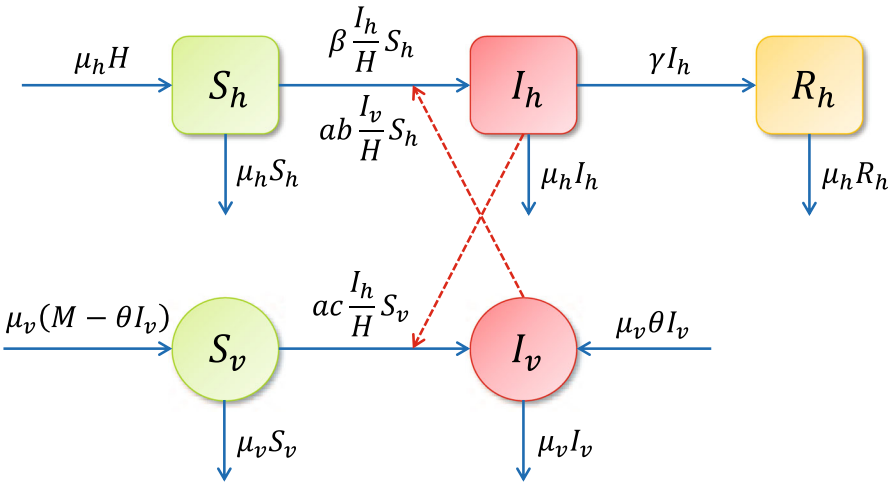

Fig. 1 Flow diagram of the Zika model

compare the role of the three routes of the model on disease transmission. In Sect. 4, we first fit the model to GBS data during 2015–2016 Zika virus epidemic in northeastern Brazil. Then, we perform sensitivity analysis with respect to the basic reproduction number and numerical simulations to investigate the role of extra transmission routes. Lastly, we draw some conclusions and discuss future work.

2 Model Formulation

To capture the essential features of Zika transmission in a simple way, we split the total human population H into susceptible humans S_h, infectious humans I_h, and recovered humans R_h. Meanwhile, the total mosquito population M is divided into susceptible mosquitoes S_v and infectious mosquitoes I_v. Incubation periods of viruses within humans and mosquitoes are ignored. We assume that birth and death rates of humans are balanced, and all newborn babies are susceptible. A susceptible human becomes infected through the bite of an infectious mosquito or sexual contact with an infected partner. Vertical transmission in humans is neglected because the infectious period of Zika is short compared to human longevity and newborns make no contribution to sexual or vertical transmission (Olawoyin and Kribs 2018). Patients who recover from the disease are conferred permanent immunity against reinfection. Since the symptoms of Zika are subclinical or mild and rarely fatal, we omit the disease-caused mortality in humans. For mosquitoes, we similarly assume that their birth and mortality rates are equal. Vertical transmission from mother to offspring and vectorial transmission from hosts to vectors are considered. Infected mosquitoes do not recover due to their short lifespan.

Based on the above assumptions and the flow diagram in Fig. 1, we arrive at the following system of ordinary differential equations with nonnegative initial conditions to describe the transmission dynamics of Zika virus between humans and mosquitoes

Table 1 Descriptions and ranges of model parameters

	Description	Range	References
a	Mosquitoes biting rate (number of bites per mosquito per day)	0.3−1.0	[1,5]
b	Transmission probability from an infectious mosquito to a susceptible human per bite (dimensionless)	0.1−0.75	[1]
c	Transmission probability from an infectious human to a susceptible mosquito per bite (dimensionless)	0.3−0.75	[2]
β	Transmission coefficient from infected humans to susceptible humans (per day)	0.001−0.1	[3]
γ	Recovery rate of humans (per day)	0.07−0.30	[8]
μ_h	Mortality rate of humans (per day)	3.65×10^{-5} –4.98×10^{-5}	[7]
μ_v	Mortality rate of mosquitoes (per day)	0.029−0.25	[1,2]
θ	Proportion of congenital infections in the offspring of infected female mosquitoes (dimensionless)	0−0.004	[4,9]
m	Ratio of mosquitoes to humans (mosquitoes per human)	1−10	[3,6]

The references are: 1- Andraud et al. (2012), 2- Chikaki and Ishikawa (2009), 3- Gao et al. (2016), 4- Lai et al. (2020), 5- Manore et al. (2014), 6- de Castro Medeiros et al. (2011), 7- Roser et al. (2019), 8- Shutt et al. (2017), and 9- Thangamani et al. (2016)

$$\begin{aligned}
\frac{\mathrm{d}S_h}{\mathrm{d}t} &= -\left(ab\frac{I_v}{H}S_h + \beta\frac{I_h}{H}S_h\right) + \mu_h(H - S_h),\\
\frac{\mathrm{d}I_h}{\mathrm{d}t} &= \left(ab\frac{I_v}{H}S_h + \beta\frac{I_h}{H}S_h\right) - (\gamma + \mu_h)I_h,\\
\frac{\mathrm{d}R_h}{\mathrm{d}t} &= \gamma I_h - \mu_h R_h,\\
\frac{\mathrm{d}S_v}{\mathrm{d}t} &= -ac\frac{I_h}{H}S_v + \mu_v(M - S_v - \theta I_v),\\
\frac{\mathrm{d}I_v}{\mathrm{d}t} &= ac\frac{I_h}{H}S_v - \mu_v(1-\theta)I_v.
\end{aligned} \tag{1}$$

Here, a is the mosquito biting rate, b and c are the transmission probabilities from an infectious mosquito to a susceptible human and from an infectious human to a susceptible mosquito per bite, respectively, β is the transmission coefficient from infected humans to susceptible humans, γ is the human recovery rate, μ_h and μ_v denote the mortality rates of humans and mosquitoes, respectively, and θ is the proportion of congenital infections in the offspring of infected female mosquitoes. Until otherwise stated, all model parameters are positive constants. According to the epidemiology of Zika, the ranges of parameters involved in model (1) are summarized in Table 1.

Since the total human and mosquito populations, $H = S_h + I_h + R_h$ and $M = S_v + I_v$, are constant, system (1) can be reduced to an equivalent system

$$\frac{\mathrm{d}I_h}{\mathrm{d}t} = \left(ab\frac{I_v}{H} + \beta\frac{I_h}{H}\right)(H - I_h - R_h) - (\gamma + \mu_h)I_h,$$

$$\begin{aligned}\frac{\mathrm{d}R_h}{\mathrm{d}t} &= \gamma I_h - \mu_h R_h,\\ \frac{\mathrm{d}I_v}{\mathrm{d}t} &= ac\frac{I_h}{H}(M - I_v) - \mu_v(1-\theta)I_v.\end{aligned} \tag{2}$$

Clearly, system (2) is mathematically well-posed and biologically meaningful.

Theorem 1 *System* (2) *has a unique solution for all time* $t \geq 0$ *with initial condition lying in*

$$\Omega = \left\{(I_h, R_h, I_v) \in \mathbb{R}^3_+ \mid I_h + R_h \leq H,\ I_v \leq M\right\}.$$

Moreover, Ω *is a positively invariant set of system* (2).

Proof Since the vector field generated by the right side of (2) is continuously differentiable in Ω, there exists a unique solution for all time $t \geq 0$. If $I_h = 0$, then $I_h' \geq 0$. Similarly, we can get the relationship about R_h and I_v. Moreover, if $I_h + R_h = H$, then $I_h' + R_h' \leq 0$; if $I_v = M$, then $I_v' \leq 0$. We have thus proved the positive invariance of Ω (i.e., the solutions starting in Ω remain in Ω for all time t). □

3 Mathematical Analysis

In this section, we first calculate the basic reproduction number of model (2), and then investigate the threshold dynamics of the model. The relative contributions of each transmission mode on the basic reproduction number and host infection size are analyzed at the end.

3.1 Basic Reproduction Number

It is easy to see that system (2) has a unique disease-free equilibrium (DFE) at $E_0 = (0, 0, 0)$. Using the next-generation matrix method (Diekmann et al. 1990; van den Driessche and Watmough 2002), the rates of appearance of new infections and transition of individuals are

$$\mathscr{F} = \begin{pmatrix} \left(ab\frac{I_v}{H} + \beta\frac{I_h}{H}\right)(H - I_h - R_h) \\ ac\frac{I_h}{H}(M - I_v) + \mu_v\theta I_v \end{pmatrix} \quad \text{and} \quad \mathscr{V} = \begin{pmatrix} (\gamma + \mu_h)I_h \\ \mu_v I_v \end{pmatrix},$$

respectively. So, the new incidence and transition matrices are

$$F = \begin{pmatrix} \beta & ab \\ ac\dfrac{M}{H} & \mu_v\theta \end{pmatrix} \quad \text{and} \quad V = \begin{pmatrix} \gamma + \mu_h & 0 \\ 0 & \mu_v \end{pmatrix},$$

respectively. Thus, the characteristic equation of the next generation matrix FV^{-1} is

$$\lambda^2 - (\mathcal{R}_{hh} + \mathcal{R}_{vv})\lambda + (\mathcal{R}_{hh}\mathcal{R}_{vv} - \mathcal{R}_{hv}^2) = 0,$$

where

$$\mathcal{R}_{hh} = \frac{\beta}{\gamma + \mu_h}, \quad \mathcal{R}_{hv} = \sqrt{\frac{a^2 bcM}{\mu_v(\gamma + \mu_h)H}} \quad \text{and} \quad \mathcal{R}_{vv} = \theta$$

are the reproduction numbers caused by sexual transmission, vector-borne transmission and vertical transmission, respectively. Hence, the basic reproduction number of model (2) is

$$\begin{aligned} \mathcal{R}_0 &= \rho(FV^{-1}) \\ &= \frac{1}{2}\left(\mathcal{R}_{hh} + \mathcal{R}_{vv} + \sqrt{(\mathcal{R}_{hh} - \mathcal{R}_{vv})^2 + 4\mathcal{R}_{hv}^2}\right) \\ &= \frac{1}{2}\left(\frac{\beta}{\gamma + \mu_h} + \theta + \sqrt{\left(\frac{\beta}{\gamma + \mu_h} - \theta\right)^2 + \frac{4a^2 bcM}{\mu_v(\gamma + \mu_h)H}}\right). \end{aligned} \tag{3}$$

Obviously, $\mathcal{R}_0 > \max\{\mathcal{R}_{hv}, \mathcal{R}_{hh}, \mathcal{R}_{vv}\}$, which means that the presence of sexual transmission and vertical transmission increases the risk of infection.

Theorem 2 *For system (2), the disease-free equilibrium E_0 is globally asymptotically stable in Ω if $\mathcal{R}_0 \leq 1$, and unstable otherwise.*

Proof It is straightforward to obtain the local stability properties of E_0 by applying Theorem 2 in van den Driessche and Watmough (2002). Next, we prove the global attractivity of the disease-free equilibrium E_0 as $\mathcal{R}_0 \leq 1$. It follows from $I_h + R_h \leq H$ and $I_v \leq M$ that

$$\begin{aligned} \frac{\mathrm{d}I_h}{\mathrm{d}t} &\leq (abI_v + \beta I_h) - (\gamma + \mu_h)I_h, \\ \frac{\mathrm{d}I_v}{\mathrm{d}t} &\leq ac\frac{M}{H}I_h - \mu_v(1 - \theta)I_v, \end{aligned}$$

or equivalently,

$$\left(\frac{\mathrm{d}I_h}{\mathrm{d}t}, \frac{\mathrm{d}I_v}{\mathrm{d}t}\right)^{\mathrm{T}} \leq \begin{pmatrix} \beta - \gamma - \mu_h & ab \\ ac\dfrac{M}{H} & -\mu_v(1 - \theta) \end{pmatrix} \begin{pmatrix} I_h \\ I_v \end{pmatrix} = (F - V) \begin{pmatrix} I_h \\ I_v \end{pmatrix}.$$

The facts that the matrix $V^{-1}F$ is nonnegative and irreducible and $\mathcal{R}_0 = \rho(FV^{-1}) = \rho(V^{-1}F)$ imply that there exists a positive left eigenvector $\boldsymbol{\nu}$ such that

$$\boldsymbol{\nu} V^{-1} F = \mathcal{R}_0 \boldsymbol{\nu}.$$

Consider a Lyapunov function

$$L_0(I_h, I_v) = \boldsymbol{\nu} V^{-1}(I_h, I_v)^{\mathrm{T}}.$$

Differentiating L_0 along the trajectories of (2) gives

$$\begin{aligned}\frac{\mathrm{d}L_0}{\mathrm{d}t} &= \boldsymbol{\nu} V^{-1}\left(\frac{\mathrm{d}I_h}{\mathrm{d}t}, \frac{\mathrm{d}I_v}{\mathrm{d}t}\right)^{\mathrm{T}} \le \boldsymbol{\nu} V^{-1}(F - V)(I_h, I_v)^{\mathrm{T}} \\ &= (\mathcal{R}_0 - 1)\boldsymbol{\nu}(I_h, I_v)^{\mathrm{T}}.\end{aligned}$$

If $\mathcal{R}_0 < 1$, then $L_0' = 0$ implies that $I_h = I_v = 0$. The second equation of (2) gives $R_h' = -\mu_h R_h$ and thus $R_h = 0$; if $\mathcal{R}_0 = 1$, the equality $L_0' = 0$ implies that

$$\left(\frac{\mathrm{d}I_h}{\mathrm{d}t}, \frac{\mathrm{d}I_v}{\mathrm{d}t}\right)^{\mathrm{T}} = (F - V)(I_h, I_v)^{\mathrm{T}},$$

i.e.,

$$\begin{aligned}&\left(ab\frac{I_v}{H} + \beta\frac{I_h}{H}\right)(H - I_h - R_h) = abI_v + \beta I_h, \\ &\frac{I_h}{H}(M - I_v) = \frac{I_h}{H}M.\end{aligned} \tag{4}$$

From the second equation of (4), we conclude that $I_h = 0$ or $I_v = 0$. If $I_h = 0$, then $R_h' = -\mu_h R_h$ and $I_v' = -\mu_v(1-\theta)I_v$. Hence $R_h = I_v = 0$. If $I_v = 0$, then the first equation of (4) gives $\beta\frac{I_h}{H}(H - I_h - R_h) = \beta I_h$, which implies $I_h = 0$ and thus we can again get $R_h = I_v = 0$.

In conclusion, if $\mathcal{R}_0 \le 1$, the largest invariant set contained in $\{(I_h, R_h, I_v) \in \Omega : L_0' = 0\}$ is the singleton $\{E_0\}$. By LaSalle's invariance principle (Lasalle 1976), the disease-free equilibrium E_0 is globally asymptotically stable in Ω when $\mathcal{R}_0 \le 1$. □

3.2 Endemic Equilibrium

Besides the disease-free equilibrium, model (2) can have an endemic equilibrium $E^* = (I_h^*, R_h^*, I_v^*)$ as $\mathcal{R}_0 > 1$, which satisfies

$$\begin{aligned}&\left(ab\frac{I_v^*}{H} + \beta\frac{I_h^*}{H}\right)(H - I_h^* - R_h^*) - (\gamma + \mu_h)I_h^* = 0, \\ &\gamma I_h^* - \mu_h R_h^* = 0, \\ &ac\frac{I_h^*}{H}(M - I_v^*) - \mu_v(1-\theta)I_v^* = 0.\end{aligned} \tag{5}$$

Solving R_h^* and I_v^* from the second and third equations of (5) gives

$$R_h^* = \frac{\gamma}{\mu_h} I_h^* \quad \text{and} \quad I_v^* = \frac{acM}{acI_h^* + \mu_v(1-\theta)H} I_h^*,$$

respectively, and substituting them into the first equation of (5) gives

$$\left(ab \frac{acM}{acI_h^* + \mu_v(1-\theta)H} \frac{I_h^*}{H} + \beta \frac{I_h^*}{H} \right) (H - I_h^* - \frac{\gamma}{\mu_h} I_h^*) - (\gamma + \mu_h) I_h^* = 0.$$

After a straightforward but tedious manipulation, the above equation can be simplified to

$$c_2 (I_h^*)^2 + c_1 I_h^* + c_0 = 0,$$

where

$$\begin{aligned}
c_2 &= ac\beta(\gamma + \mu_h), \\
c_1 &= a^2 bcM(\gamma + \mu_h) - ac\mu_h(\beta - \gamma - \mu_h)H + \beta\mu_v(1-\theta)(\gamma + \mu_h)H, \\
c_0 &= -H\mu_h(a^2 bcM + \mu_v(1-\theta)(\beta - \gamma - \mu_h)H).
\end{aligned}$$

Clearly, $c_2 > 0$. According to the definition of $\mathcal{R}_0$, it follows that c_0 and $\mathcal{R}_0 - 1$ have opposite signs. Indeed, note that $1 - \mathcal{R}_{vv} = 1 - \theta \geq 0$ and

$$\begin{aligned}
\operatorname{sgn}(c_0) &= -\operatorname{sgn}\left(\frac{a^2 bcM}{\mu_v(\gamma + \mu_h)H} + \frac{\mu_v(1-\theta)(\beta - \gamma - \mu_h)H}{\mu_v(\gamma + \mu_h)H} \right) \\
&= -\operatorname{sgn}(\mathcal{R}_{hv}^2 + (1 - \mathcal{R}_{vv})(\mathcal{R}_{hh} - 1)).
\end{aligned}$$

If $\mathcal{R}_{hh} < 1$, then

$$\begin{aligned}
c_0 < 0 &\Leftrightarrow \mathcal{R}_{hv}^2 + (1 - \mathcal{R}_{vv})(\mathcal{R}_{hh} - 1) > 0 \\
&\Leftrightarrow 4\mathcal{R}_{hv}^2 + ((\mathcal{R}_{hh} - 1) + (1 - \mathcal{R}_{vv}))^2 > ((1 - \mathcal{R}_{hh}) + (1 - \mathcal{R}_{vv}))^2 \\
&\Leftrightarrow (\mathcal{R}_{hh} - \mathcal{R}_{vv})^2 + 4\mathcal{R}_{hv}^2 > (2 - \mathcal{R}_{hh} - \mathcal{R}_{vv})^2 \\
&\Leftrightarrow \sqrt{(\mathcal{R}_{hh} - \mathcal{R}_{vv})^2 + 4\mathcal{R}_{hv}^2} > |2 - \mathcal{R}_{hh} - \mathcal{R}_{vv}| = 2 - \mathcal{R}_{hh} - \mathcal{R}_{vv} \\
&\Leftrightarrow \mathcal{R}_0 = \frac{1}{2}\left(\mathcal{R}_{hh} + \mathcal{R}_{vv} + \sqrt{(\mathcal{R}_{hh} - \mathcal{R}_{vv})^2 + 4\mathcal{R}_{hv}^2} \right) > 1.
\end{aligned}$$

If $\mathcal{R}_{hh} \geq 1$, then $c_0 < 0$ and $\mathcal{R}_0 > \mathcal{R}_{hh} \geq 1$. This conclusion can be easily seen from another threshold quantity $\widetilde{\mathcal{R}}_0$ defined in Sect. 3.3.

We are now ready to establish the following result on the existence and local stability of the endemic equilibrium. The proof is postponed to Appendix A.

Theorem 3 *For system (2), there exists a unique endemic equilibrium* $E^* = (I_h^*, R_h^*, I_v^*)$ *if and only if* $\mathcal{R}_0 > 1$. *Moreover,* E^* *is locally asymptotically stable.*

In what follows, we prove that the disease persists in the host population when $\mathcal{R}_0 > 1$. So the basic reproduction number $\mathcal{R}_0$ is a sharp threshold for disease persistence and extinction.

Theorem 4 *For model (2), if $\mathcal{R}_0 > 1$, then the disease is uniformly persistent as long as it initially presents. Namely, there exists a constant $\varepsilon > 0$ such that each solution $\varphi_t(\boldsymbol{x}_0) = (I_h(t), R_h(t), I_v(t))$ with the initial value $\boldsymbol{x}_0 = (I_h(0), R_h(0), I_v(0))$ in the interior of Ω satisfies*

$$\liminf_{t\to\infty} (I_h(t), I_v(t)) \gg (\varepsilon, \varepsilon).$$

Proof First, we define

$$\begin{aligned}
\mathring{\Omega} &= \{(I_h, R_h, I_v) \in \Omega \mid I_h > 0,\ I_v > 0\},\\
\partial\Omega &= \Omega\backslash\mathring{\Omega} = \{(I_h, R_h, I_v) \in \Omega \mid I_h = 0 \text{ or } I_v = 0\}.
\end{aligned}$$

Clearly, both Ω and $\mathring{\Omega}$ are positively invariant and the set $\partial\Omega$ is relatively closed in Ω. The compactness and positive invariance of Ω imply that system (2) is point dissipative. It suffices to prove that system (2) is uniformly persistent with respect to $(\mathring{\Omega}, \partial\Omega)$. Define

$$\begin{aligned}
\Gamma &= \{\boldsymbol{x}_0 \in \partial\Omega : \varphi_t(\boldsymbol{x}_0) \in \partial\Omega,\ \forall\, t > 0\},\\
D &= \{(I_h, R_h, I_v) \in \Omega \mid I_h = 0,\ I_v = 0\}.
\end{aligned}$$

It is easy to see that $D \subseteq \Gamma \subseteq \partial\Omega$. For any $\boldsymbol{x}_0 \in \partial\Omega\backslash D$, it follows from the fact

$$\begin{aligned}
I_h(t) =& e^{-(\gamma+\mu_h)t}\left(I_h(0) + \int_0^t \left(ab\frac{I_v(s)}{H} + \beta\frac{I_h(s)}{H}\right)\right.\\
&\left.\times (H - I_h(s) - R_h(s))e^{(\gamma+\mu_h)s}ds\right) > 0,\\
R_h(t) =& e^{-\mu_h t}\left(R_h(0) + \int_0^t \gamma I_h(s)e^{\mu_h s}ds\right) > 0,\\
I_v(t) =& e^{-\mu_v(1-\theta)t}\left(I_v(0) + \int_0^t ac\frac{I_h(s)}{H}(M - I_v(s))e^{\mu_v(1-\theta)s}ds\right) > 0,
\end{aligned}$$

that $\varphi_t(\boldsymbol{x}_0) \in \mathring{\Omega}$ for all $t > 0$ and hence $\boldsymbol{x}_0 \notin \Gamma$. Thus, we have $\Gamma \subseteq D$ and $\Gamma = D$. Moreover, $\bigcup_{\boldsymbol{x}_0\in\Gamma} \omega(\boldsymbol{x}_0) = \{E_0\}$. By Theorem 4.6 in Thieme (1993), it only remains to show that $W^s(E_0) \bigcap \mathring{\Omega} = \emptyset$, where $W^s(E_0)$ denotes the stable manifold of E_0.

Assume the contrary, there exists $\boldsymbol{x}_0 \in \mathring{\Omega}$ such that $\varphi_t(\boldsymbol{x}_0) \to E_0$ as $t \to +\infty$. Denote

$$J(\eta) = F - V - \eta G$$
$$= \begin{pmatrix} \beta\dfrac{H-2\eta}{H} - \gamma - \mu_h & \dfrac{ab(H-2\eta)}{H} \\ \dfrac{ac(M-\eta)}{H} & -\mu_v(1-\theta) \end{pmatrix} \text{ with } G = \begin{pmatrix} \dfrac{2\beta}{H} & \dfrac{2ab}{H} \\ \dfrac{ac}{H} & 0 \end{pmatrix}.$$

By Theorem 2 in van den Driessche and Watmough (2002), the spectral bound of $F - V$, denoted by $s(F - V) = s(J(0))$, is positive if and only if $\mathcal{R}_0 > 1$. Since $s(J(\eta))$ is continuous for small η, there exists a small enough $\eta_1 > 0$ such that $s(J(\eta)) > 0$ for $\eta \in [0, \eta_1]$. Meanwhile, up to a translation, we have

$$\|\varphi_t(\boldsymbol{x}_0) - E_0\|_2 = \|\varphi_t(\boldsymbol{x}_0)\|_2 \leq \eta_1, \ \forall\, t \geq 0, \tag{6}$$

where $\|\cdot\|_2$ is the usual Euclidean norm. Therefore,

$$\left(\frac{\mathrm{d}I_h}{\mathrm{d}t}, \frac{\mathrm{d}I_v}{\mathrm{d}t}\right)^{\mathrm{T}} \geq J(\eta_1)(I_h, I_v)^{\mathrm{T}}.$$

Since $J(\eta_1)$ is irreducible and essentially nonnegative, it has a positive eigenvector associated with $s(J(\eta_1)) > 0$. By a simple comparison principle, $I_h(t) \to +\infty$ and $I_v(t) \to +\infty$ as $t \to +\infty$, contradicting (6). Note that the singleton $\{E_0\}$ is an isolated invariant set and acyclic. The uniform persistence of system (2) in $\mathring{\Omega}$ as $\mathcal{R}_0 > 1$ can be concluded from Theorem 4.6 in Thieme (1993). □

Before ending this subsection, we show the global attractivity of the endemic equilibrium which generalizes the important work of Souza (2014).

Theorem 5 *For model (2), if $\mathcal{R}_0 > 1$, then the unique endemic equilibrium E^* is globally asymptotically stable.*

Proof We construct a Lyapunov function to prove the global asymptotic stability of the endemic equilibrium. Introducing the change of variables

$$X = \frac{S_h}{H}, \quad Y = \frac{I_h}{H}, \quad \text{and} \quad Z = \frac{I_v}{M},$$

simplifies (1) to the following topologically equivalent system

$$\begin{aligned} \frac{\mathrm{d}X}{\mathrm{d}t} &= -\left(\tilde{b}XZ + \beta XY\right) + \mu_h(1 - X), \\ \frac{\mathrm{d}Y}{\mathrm{d}t} &= \left(\tilde{b}XZ + \beta XY\right) - \tilde{\gamma}Y, \\ \frac{\mathrm{d}Z}{\mathrm{d}t} &= \tilde{c}(1 - Z)Y - \tilde{\mu}_v Z, \end{aligned} \tag{7}$$

where

$$\tilde{b} = abm, \quad \tilde{\gamma} = \gamma + \mu_h, \quad \tilde{c} = ac \quad \text{and} \quad \tilde{\mu}_v = \mu_v(1 - \theta).$$

Let (X^*, Y^*, Z^*) be the unique endemic equilibrium of system (7). The equilibrium equations of system (7) lead to

$$\mu_h = \tilde{b}X^*Z^* + \beta X^*Y^* + \mu_h X^*, \tag{8a}$$
$$\tilde{\gamma}Y^* = \tilde{b}X^*Z^* + \beta X^*Y^*, \tag{8b}$$
$$\tilde{\mu}_v Z^* = \tilde{c}(1 - Z^*)Y^*. \tag{8c}$$

Define

$$L_1 = X^* g\left(\frac{X}{X^*}\right), \quad L_2 = Y^* g\left(\frac{Y}{Y^*}\right) \quad \text{and} \quad L_3 = \frac{\tilde{b}X^*Z^*}{\tilde{\mu}_v} g\left(\frac{Z}{Z^*}\right),$$

where $g(\xi) = \xi - 1 - \ln\xi \geq 0$ with equality if and only if $\xi = 1$. By using (8a),

$$\begin{aligned}
L_1' &= \left(1 - \frac{X^*}{X}\right)\left(-\left(\tilde{b}XZ + \beta XY\right) + \mu_h(1 - X)\right) \\
&= \left(1 - \frac{X^*}{X}\right)\left(-\tilde{b}XZ - \beta XY - \mu_h X + \tilde{b}X^*Z^* + \beta X^*Y^* + \mu_h X^*\right) \\
&= -\frac{\mu_h}{X}(X - X^*)^2 + \tilde{b}X^*Z^*\left(1 - \frac{X^*}{X} - \frac{XZ}{X^*Z^*} + \frac{Z}{Z^*}\right) \\
&\quad + \beta X^*Y^*\left(1 - \frac{X^*}{X} - \frac{XY}{X^*Y^*} + \frac{Y}{Y^*}\right).
\end{aligned}$$

Similarly, by applying (8b),

$$\begin{aligned}
L_2' &= \left(1 - \frac{Y^*}{Y}\right)\left(\tilde{b}XZ + \beta XY - \tilde{\gamma}Y\right) \\
&= \left(1 - \frac{Y^*}{Y}\right)\left(\tilde{b}XZ + \beta XY - \left(\tilde{b}X^*Z^* + \beta X^*Y^*\right)\frac{Y}{Y^*}\right) \\
&= \tilde{b}X^*Z^*\left(\frac{XZ}{X^*Z^*} - \frac{Y^*XZ}{YX^*Z^*} - \frac{Y}{Y^*} + 1\right) \\
&\quad + \beta X^*Y^*\left(\frac{XY}{X^*Y^*} - \frac{X}{X^*} - \frac{Y}{Y^*} + 1\right),
\end{aligned}$$

and by (8c),

$$\begin{aligned}
L_3' &= \frac{\tilde{b}X^*}{\tilde{\mu}_v}\left(1 - \frac{Z^*}{Z}\right)(\tilde{c}(1 - Z)Y - \tilde{\mu}_v Z) \\
&= \frac{\tilde{b}X^*}{\tilde{\mu}_v}\left(1 - \frac{Z^*}{Z}\right)\left(\tilde{c}(1 - Z^*)Y + \tilde{c}(Z^* - Z)Y - \tilde{\mu}_v Z\right) \\
&= -\frac{\tilde{b}X^*\tilde{c}Y}{\tilde{\mu}_v Z}(Z - Z^*)^2 + \frac{\tilde{b}X^*Z^*}{\tilde{\mu}_v Z^*}\left(1 - \frac{Z^*}{Z}\right)\left(\tilde{c}(1 - Z^*)Y - \tilde{\mu}_v Z\right)
\end{aligned}$$

$$= -\frac{\tilde{b}X^*\tilde{c}Y}{\tilde{\mu}_v Z}(Z-Z^*)^2 + \tilde{b}X^*Z^*\left(\frac{Y}{Y^*} - \frac{YZ^*}{Y^*Z} - \frac{Z}{Z^*} + 1\right).$$

Consider a Lyapunov function $L = L_1 + L_2 + L_3$. Then,

$$\begin{aligned}
L' =& L_1' + L_2' + L_3' \\
=& -\frac{\mu_h}{X}(X-X^*)^2 - \frac{\tilde{b}X^*\tilde{c}Y}{\tilde{\mu}_v Z}(Z-Z^*)^2 \\
&+ \tilde{b}X^*Z^*\left(1 - \frac{X^*}{X} - \frac{XZ}{X^*Z^*} + \frac{Z}{Z^*}\right) \\
&+ \tilde{b}X^*Z^*\left(\frac{XZ}{X^*Z^*} - \frac{Y^*XZ}{YX^*Z^*} - \frac{Y}{Y^*} + 1\right) \\
&+ \tilde{b}X^*Z^*\left(\frac{Y}{Y^*} - \frac{YZ^*}{Y^*Z} - \frac{Z}{Z^*} + 1\right) \\
&+ \beta X^*Y^*\left(1 - \frac{X^*}{X} - \frac{XY}{X^*Y^*} + \frac{Y}{Y^*}\right) \\
&+ \beta X^*Y^*\left(\frac{XY}{X^*Y^*} - \frac{X}{X^*} - \frac{Y}{Y^*} + 1\right) \\
=& -\frac{\mu_h}{X}(X-X^*)^2 - \frac{\tilde{b}X^*\tilde{c}Y}{\tilde{\mu}_v Z}(Z-Z^*)^2 \\
&+ \tilde{b}X^*Z^*\left(3 - \frac{X^*}{X} - \frac{Y^*XZ}{YX^*Z^*} - \frac{YZ^*}{Y^*Z}\right) + \beta X^*Y^*\left(2 - \frac{X^*}{X} - \frac{X}{X^*}\right).
\end{aligned}$$

Using the inequality of arithmetic and geometric means, we can get $L' \leq 0$ with equality if and only if $(X, Y, Z) = (X^*, Y^*, Z^*)$. Hence, the endemic equilibrium is globally asymptotically stable whenever $\mathcal{R}_0 > 1$. □

3.3 Relative Contribution

The basic reproduction number $\mathcal{R}_0$ defined in (3) takes a complicated form that makes it difficult to compare the relative contribution of different transmission routes. Thus, we redefine the basic reproduction number in a way similar to that of Section 12.4 in Brauer et al. (2019) or Brauer et al. (2016). Namely, only host infection is regarded as new infection, while vector infection is viewed as transition. If so, then the rates of appearance of new infections and transition of individuals are

$$\widetilde{\mathscr{F}} = \begin{pmatrix} ab\frac{I_v}{H}S_h + \beta\frac{I_h}{H}S_h \\ 0 \end{pmatrix} \quad \text{and} \quad \widetilde{\mathscr{V}} = \begin{pmatrix} (\gamma+\mu_h)I_h \\ -ac\frac{I_h}{H}S_v + \mu_v(1-\theta)I_v \end{pmatrix},$$

respectively. Thus, the new incidence and transition matrices are

$$\widetilde{F} = \begin{pmatrix} \beta & ab \\ 0 & 0 \end{pmatrix} \quad \text{and} \quad \widetilde{V} = \begin{pmatrix} \gamma + \mu_h & 0 \\ -ac\dfrac{M}{H} & \mu_v(1-\theta) \end{pmatrix},$$

respectively. The basic reproduction number of model (1) is now defined as

$$\begin{aligned} \widetilde{\mathcal{R}}_0 = \rho(\widetilde{F}\widetilde{V}^{-1}) =& \frac{\beta}{\gamma+\mu_h} + \frac{a^2bcM}{(\gamma+\mu_h)\mu_v H}\left(1+\frac{\theta}{1-\theta}\right) \\ =& \widetilde{\mathcal{R}}_{hh} + \widetilde{\mathcal{R}}_{hv} + \widetilde{\mathcal{R}}_{vv}, \end{aligned}$$

where

$$\widetilde{\mathcal{R}}_{hh} = \frac{\beta}{\gamma+\mu_h}, \quad \widetilde{\mathcal{R}}_{hv} = \frac{a^2bcM}{(\gamma+\mu_h)\mu_v H}, \quad \text{and} \quad \widetilde{\mathcal{R}}_{vv} = \frac{a^2bcM}{(\gamma+\mu_h)\mu_v H}\sum_{i=1}^{\infty}\theta^i$$

are the reproduction numbers attributed to sexual transmission, vector-borne transmission and vertical transmission, respectively. Since $\mathrm{sgn}(\widetilde{\mathcal{R}}_0 - 1) = \mathrm{sgn}(s(\widetilde{F} - \widetilde{V})) = \mathrm{sgn}(s(F - V)) = \mathrm{sgn}(\mathcal{R}_0 - 1)$, both $\widetilde{\mathcal{R}}_0$ and $\mathcal{R}_0$ are thresholds for disease extinction and persistence. The respective percentages of contribution of three transmission mechanisms to $\widetilde{\mathcal{R}}_0$ are

$$\widetilde{P}_s := \frac{\widetilde{\mathcal{R}}_{hh}}{\widetilde{\mathcal{R}}_0}, \quad \widetilde{P}_m := \frac{\widetilde{\mathcal{R}}_{hv}}{\widetilde{\mathcal{R}}_0}, \quad \text{and} \quad \widetilde{P}_v := \frac{\widetilde{\mathcal{R}}_{vv}}{\widetilde{\mathcal{R}}_0}.$$

Next, we consider the relative contribution of three transmission routes on the number of new infected humans. According to the first equation of (2), the infection rates of humans through sexual transmission and vectorial transmission at time t are

$$\beta\frac{I_h(t)}{H}(H - I_h(t) - R_h(t)) \quad \text{and} \quad ab\frac{I_v(t)}{H}(H - I_h(t) - R_h(t)),$$

respectively. By the third equation of (2), the infection rates of mosquitoes through vectorial transmission and vertical transmission at time t are

$$ac\frac{I_h(t)}{H}(M - I_v(t)) \text{ and } \theta\mu_v I_v(t),$$

respectively. The respective percentages of instantaneous host infections due to sexual transmission, vector-borne transmission and vertical transmission at time t are

$$\begin{aligned} P_s(t) :=& \frac{\beta \frac{I_h(t)}{H}(H - I_h(t) - R_h(t))}{ab\frac{I_v(t)}{H}(H - I_h(t) - R_h(t)) + \beta \frac{I_h(t)}{H}(H - I_h(t) - R_h(t))} \\ =& \frac{\beta I_h(t)}{abI_v(t) + \beta I_h(t)}, \\ P_m(t) :=& \frac{abI_v(t)}{abI_v(t) + \beta I_h(t)} \cdot \frac{ac\frac{I_h(t)}{H}(M - I_v(t))}{ac\frac{I_h(t)}{H}(M - I_v(t)) + \theta\mu_v I_v(t)}, \\ P_v(t) :=& \frac{abI_v(t)}{abI_v(t) + \beta I_h(t)} \cdot \frac{\theta\mu_v I_v(t)}{ac\frac{I_h(t)}{H}(M - I_v(t)) + \theta\mu_v I_v(t)}. \end{aligned}$$

When the disease becomes endemic, we naturally evaluate $P_\natural(t)$ for $\natural \in \{s, m, v\}$ at the unique endemic equilibrium $E^* = (I_h^*, R_h^*, I_v^*)$ which is globally asymptotically stable, that is,

$$P_s = \frac{\beta I_h^*}{abI_v^* + \beta I_h^*}, \quad P_m = (1-\theta)\frac{abI_v^*}{abI_v^* + \beta I_h^*}, \quad \text{and} \quad P_v = \theta\frac{abI_v^*}{abI_v^* + \beta I_h^*}.$$

It is worth mentioning that in reality, $P_\natural \approx \widetilde{P}_\natural$ for all $\natural \in \{s, m, v\}$. In fact,

$$\widetilde{P}_s : \widetilde{P}_m : \widetilde{P}_v = \widetilde{\mathcal{R}}_{hh} : \widetilde{\mathcal{R}}_{hv} : \widetilde{\mathcal{R}}_{vv} = \beta : \frac{a^2bcM}{\mu_v H} : \frac{a^2bcM}{\mu_v H} \cdot \frac{\theta}{1-\theta}.$$

It follows from the second and third equations of (5) and $1/\mu_h \gg 1/\gamma$ that

$$\begin{aligned} \frac{M - I_v^*}{I_v^*} &= \frac{M}{I_v^*} - 1 = \frac{\mu_v(1-\theta)}{ac} \cdot \frac{H}{I_h^*} = \frac{\mu_v(1-\theta)}{ac} \cdot \frac{S_h^* + I_h^* + R_h^*}{I_h^*} \\ &= \frac{\mu_v(1-\theta)}{ac} \cdot \frac{1}{I_h^*}\left(S_h^* + I_h^* + \frac{\gamma}{\mu_h} I_h^*\right) > \frac{\mu_v(1-\theta)}{ac}\left(1 + \frac{\gamma}{\mu_h}\right) \gg 1 \end{aligned}$$

and hence $I_v^*/M \ll 1$. Thus, again by the third equations of (5),

$$\frac{I_v^*}{I_h^*} = \frac{acM}{\mu_v(1-\theta)H}\left(1 - \frac{I_v^*}{M}\right) \approx \frac{acM}{\mu_v(1-\theta)H}.$$

At the endemic equilibrium E^*, we have

$$\begin{aligned} P_s : P_m : P_v &= \beta I_h^* : (1-\theta)abI_v^* : \theta abI_v^* = \beta : (1-\theta)ab\frac{I_v^*}{I_h^*} : \theta ab\frac{I_v^*}{I_h^*} \\ &\approx \beta : \frac{a^2bcM}{\mu_v H} : \frac{a^2bcM}{\mu_v H} \cdot \frac{\theta}{1-\theta} = \widetilde{P}_s : \widetilde{P}_m : \widetilde{P}_v. \end{aligned}$$

So the three transmission routes play a similar role in the basic reproduction number and the new host infections at the endemic equilibrium.

4 Numerical Results

In this section, we fit the Zika model to real data, and then perform some numerical analysis to investigate the effects of multiple transmission pathways on the transmission and control of Zika virus disease. The selected parameter values are given in Table 1 which are mainly adopted from Andraud et al. (2012), Chikaki and Ishikawa (2009), Gao et al. (2016), Manore et al. (2014), Shutt et al. (2017), Olawoyin and Kribs (2018) and the references cited therein. The time is measured in day.

4.1 Data Fitting

Since people infected with ZIKV are mostly asymptomatic or have only mild flu-like illness, the under-reporting rate of Zika cases is high and varies with time and location (Shutt et al. 2017). Excess GBS cases have been confirmed to be strongly correlated to ZIKV epidemics in many countries (Mier-y-Teran-Romero et al. 2018). The typical clinical features and severity of GBS make it easy to identify and record. For example, He et al. (2020) estimated that 6.1 (95% confidence interval (CI): 5.0–8.6) GBS cases may appear per 100,000 symptomatic ZIKV infections. Due to the lack of high-quality ZIKV case data, we fit our model to the reported GBS surveillance data in the northeastern region of Brazil from January 2015 to September 2016 (de Oliveira et al. 2017). The region had been worst affected by the Zika outbreak, with 94% (95% CI: 90–97%) of an estimated 8.5 million total symptomatic cases in Brazil (Brady et al. 2019). It is interesting to note that microcephaly has also been showed to be associated with Zika virus infections (de Araújo et al. 2018). However, only one wave of microcephaly was observed in the northeastern region of Brazil, while the Zika epidemic showed clearly two waves. A paper by de Oliveira et al. (2017) discussed the possible reasons behind this inconsistence. On the other hand, GBS clearly showed two waves, thus it is used here.

Let ρ be the ratio of reported excess GBS cases to ZIKV cases, which is assumed to be a constant. Some parameter values are fixed as follows:

$$b = 0.3, \quad c = 0.4, \quad \theta = 0.0034, \quad \gamma = 0.14, \quad \mu_h = 4 \times 10^{-5}, \quad \mu_v = 0.125,$$

where the time unit is one day. The total human population is fixed but the total vector population is climate-driven. We use the open source R package POMP (partially observed Markov process, also known as hidden Markov model), and one only needs to insert the equations of the model, fix parameter values, and prior values of those parameters to be estimated, and data to be fitted. The so-called plug-and-play likelihood-based inference framework is applied to estimate the remaining parameters (He et al. 2010). The R package POMP contains a built-in function of B-spline basis function. Although we use a cubic-spline in this work as an external function, our

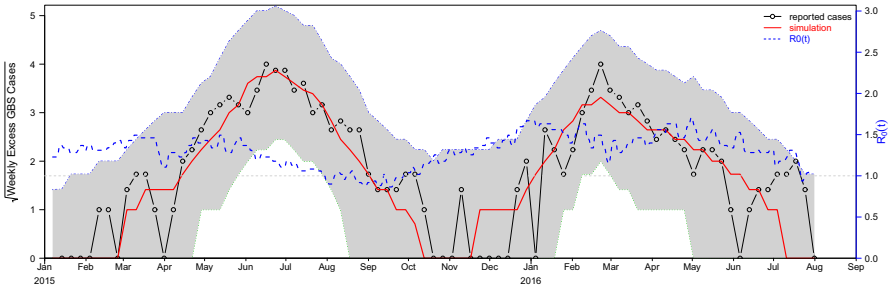

Fig. 2 Comparison of reported and simulated excess GBS cases. Black line with circles denotes the number of reported excess GBS cases, red solid line is the mean GBS cases averaged from 1000 simulations, grey shaded region is the 95% CI of the 1000 simulations, and blue dashed line shows the time evolution of $\mathcal{R}_0$ (Color figure online)

results are insensitive to this choice. For more details about the fitting process, the readers may refer to He et al. (2020) and the references therein. The fitted parameter values are $a = 0.45$, $\beta = 0.05$, and $\rho = 0.0024\%$. Figure 2 demonstrates the curve of the average GBS cases of 1000 simulations versus time which matches the trajectory of the reported GBS cases very well. The gray shaded area gives the 95% confidence interval for the number of simulated cases per day, all of which completely cover the associated observations. Thus, our model provides a good fit to the time series of the weekly reported GBS cases during and following the 2015–16 Zika virus epidemic in northeastern Brazil. Note that the current estimate of ρ is comparable but smaller than that obtained by He et al. (2020). The major reason for the difference is that we consider all infections instead of only symptomatic infections. Moreover, with the consideration of seasonal climate change, the time-varying reproduction number $\mathcal{R}_0(t)$ is estimated to vary between 0.85 and 1.71 over the study period.

4.2 Sensitivity Analysis

We now conduct sensitivity analysis of $\mathcal{R}_0$ with respect to model parameters. The frequently used sensitivity index in mathematical epidemiology is the so-called normalized forward sensitivity index, which is the ratio of the relative change in the variable to the relative change in the parameter (Arriola and Hyman 2009). Mathematically, the sensitivity index (SI) of $\mathcal{R}_0$ with respect to parameter p is defined as

$$\Upsilon_p^{\mathcal{R}_0} := \frac{\partial \mathcal{R}_0}{\partial p} \times \frac{p}{\mathcal{R}_0}.$$

Based on the fitting results in last subsection, we choose a set of baseline values for system (2) as follows (time unit is one day):

$$a = 0.45, \quad b = 0.3, \quad c = 0.4, \quad \beta = 0.05, \quad \theta = 0.0034,$$
$$\gamma = 0.14, \quad \mu_h = 4 \times 10^{-5}, \quad \mu_v = 0.125, \quad m = M/H = 1.5.$$

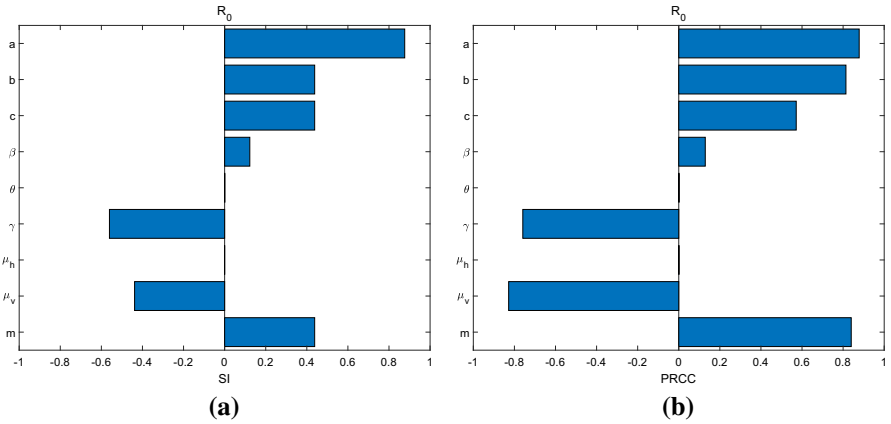

Fig. 3 Sensitivity analysis for $\mathcal{R}_0$ with model parameters: **a** sensitivity indices (SI), and **b** partial rank correlation coefficients (PRCC). See main text for parameter settings

Direct calculation gives the corresponding basic reproduction number $\mathcal{R}_0 = 1.63$. We calculate the sensitivity indices of $\mathcal{R}_0$ with respect to each model parameter which are shown in Fig. 3a. Clearly, $\mathcal{R}_0$ is much more sensitive to parameters related to mosquito-borne transmission route, e.g., a, b and c, than those of the other two transmission routes, β and θ.

Moreover, to globally quantify the uncertainty, we use the Latin hypercube sampling (LHS) method to generate 10^6 random parameter sets with parameter ranges from Table 1. Then, we compute the partial rank correlation coefficients (PRCC) of $\mathcal{R}_0$ with respect to model parameters (Marino et al. 2008) (see Fig. 3b). The reproduction number $\mathcal{R}_0$ is still most sensitive to mosquito biting rate, a, and least sensitive to proportion of congenital infections in mosquitoes, θ, human mortality rate, μ_h, and sexual transmission rate, β. However, it is also highly sensitive to the ratio of mosquitoes to humans, m, followed by mosquito mortality rate, μ_v, transmission probability from vector to host, b, and human recovery rate, γ. The results suggest that reducing exposure to vector bites and mosquito population size is essential for a successful Zika control program. Moreover, local and global sensitivity analyses on $\widetilde{\mathcal{R}}_0$ with the same parameter setting give similar results.

4.3 Numerical Simulations

Example 1 Dynamic behaviors of model system. We consider system (2) with the same parameter setting as that of the local sensitivity analysis in Sect. 4.2. In addition, the total host and vector populations are $H = 10^5$ and $M = 1.5 \times 10^5$, respectively. Recall that the associated basic reproduction number $\mathcal{R}_0 = 1.63 > 1$. For illustrative purpose only, we choose an initial condition with large fraction of hosts being recovered, i.e., $(I_h(0), R_h(0), I_v(0)) = (40, 60000, 100)$. Solution curves of $I_h(t)$ and $I_v(t)$ are shown in Fig. 4a. They slowly oscillate and converge to the unique endemic equilibrium $E^* \approx (16.9, 59098.3, 36.6)$. Hence, E^* is a stable focus, and there is a Zika epidemic

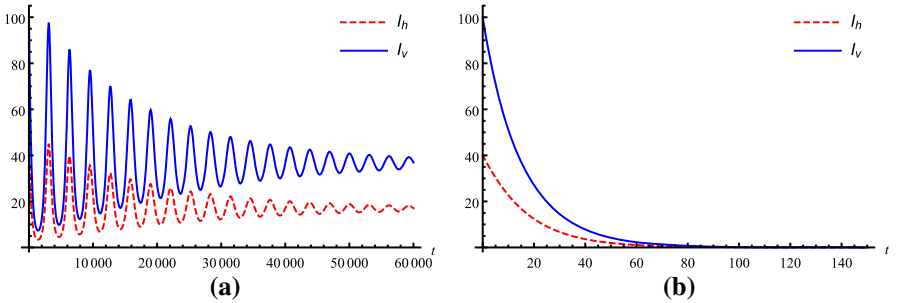

Fig. 4 Numerical solutions of system (2) with **a** $\mathcal{R}_0 = 1.63$ (the solution approaches the endemic equilibrium), and **b** $\mathcal{R}_0 = 0.92$ (the solution approaches the disease-free equilibrium). In both scenarios, the initial condition is $(I_h(0), R_h(0), I_v(0)) = (40, 60000, 100)$. See main text for parameter values and the time unit is one day

every 8–10 years. The disease persists at a low endemic level after the initial large epidemic.

Suppose people take measures, e.g., sleeping inside a mosquito net and applying mosquito repellent, to reduce mosquito bites such that there is a 50% decrease in mosquito biting rate, i.e., $a = 0.225$. Then, the basic reproduction number is calculated to be $\mathcal{R}_0 = 0.92 < 1$ when all other parameter values remain unchanged. It can be concluded from Fig. 4b that the numbers of infected humans and mosquitoes approach the disease-free equilibrium $E_0 = (0, 0, 0)$, that is, the disease dies out.

Example 2 Contribution of different transmission pathways. To demonstrate the role of each transmission pathway on host infections during the ZIKV outbreak, we set the parameter values as follows (time unit is one day):

$$a = 0.5, \quad b = 0.3, \quad c = 0.4, \quad \beta = 0.04, \quad \theta = 0.0034,$$
$$\gamma = 0.15, \quad \mu_h = 4 \times 10^{-5}, \quad \mu_v = 0.125, \quad m = 3, \quad H = 10^5.$$

The associated basic reproduction number is $\widetilde{\mathcal{R}}_0 = 5.081$ with $\widetilde{\mathcal{R}}_{hh} = 0.266$, $\widetilde{\mathcal{R}}_{hv} = 4.799$ and $\widetilde{\mathcal{R}}_{vv} = 0.016$, which gives

$$\widetilde{P}_s = 5.246\%, \quad \widetilde{P}_m = 94.432\%, \quad \text{and} \quad \widetilde{P}_v = 0.322\%.$$

Thus, there is a disease outbreak when an infected person is introduced into a totally susceptible population of hosts and vectors. The real time human infection rate and number of infected humans, i.e.,

$$\frac{\beta I_h(t) + abI_v(t)}{H}(H - I_h(t) - R_h(t)) \quad \text{and} \quad I_h(t),$$

are shown in Fig. 5a. As expected, the host infection rate reaches its peak about 5 days earlier than the host infection size. The percentage of contribution of each transmission route to the host infection rate is showed in Fig. 5b. It can be seen that the mosquito-borne transmission route swiftly plays an absolutely dominant role. Meanwhile, the

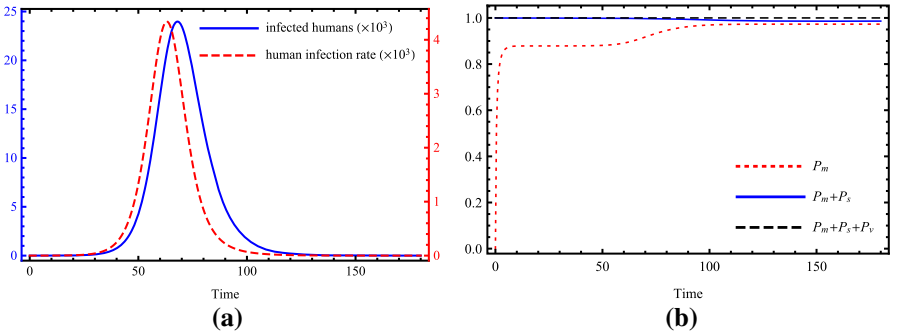

Fig. 5 **a** The number of infected humans (blue solid line with left y-axis) and the host infection rate (red dashed line with right y-axis), **b** the percentage of contribution of mosquito-borne transmission route (red dotted line), mosquito-borne and sexual transmission routes (blue solid line), and all three transmission routes (black dashed line), to the host infection rate. The initial condition is $(I_h(0), R_h(0), I_v(0)) = (1, 0, 0)$. See main text for parameter values and the time unit is one day (Color figure online)

relative contribution of sexual transmission sharply decreases and stays at a lower level until the host infection rate passes its peak and eventually decreases to an even smaller level. The relative contribution of vertical transmission in mosquitoes slowly increases from zero to an extremely small level. Moreover, if no intervention is implemented, the cumulative number of new host infections during a given time period $[0, T]$ is

$$C(T) := \int_0^T \frac{\beta I_h(t) + abI_v(t)}{H}(H - I_h(t) - R_h(t))\mathrm{d}t.$$

For the scenario showed in Fig. 5a, we have $C(180) = 98588$, of which 9.31%, 90.46% and 0.23% are contributed by sexual transmission, mosquito-borne transmission and vertical transmission, respectively. This result can also be viewed as the relative contribution of different routes to the final size when human vital dynamics are ignored.

In the long run, the disease persists at the endemic equilibrium $E^* = (21, 80294, 103)$, and the percentages of contribution of all three routes are

$$P_s = 5.248\%, \quad P_m = 94.430\%, \quad \text{and} \quad P_v = 0.322\%.$$

We can see that the role of sexual transmission in the early outbreak is greater than the long term, but vertical transmission is just the opposite. Furthermore, using the LHS method, we generate 10^5 random parameter sets with ranges followed Table 1 and obtain 99,114 sets whose corresponding $\widetilde{\mathcal{R}}_0 > 1$. For these qualified scenarios, the medians of the distributions of the percentage of contribution from sexual, mosquito-borne, and vertical transmission mechanisms are

$$1.4\%, \quad 98.4\%, \quad \text{and} \quad 0.2\%,$$

respectively, in both $\widetilde{\mathcal{R}}_0$ and long-term new host infections.

5 Discussion

In this paper, we formulated a new mathematical model for the dynamical transmission of Zika virus disease. Our model incorporates three transmission modes, that is, vectorial transmission, sexual transmission and vertical transmission. The human population is divided into three classes, namely susceptible, infectious and recovered, while the mosquito population is divided into two classes, namely susceptible and infectious. We derived the basic reproduction number $\mathcal{R}_0$ and analyzed the dynamical behavior of the system. Specifically, the disease-free equilibrium E_0 is globally asymptotically stable when $\mathcal{R}_0 \leq 1$, whereas the disease is uniformly persistent, and there exists a unique endemic equilibrium which is globally asymptotically stable when $\mathcal{R}_0 > 1$. By treating new mosquito infections as state transition, we defined a new basic reproduction number $\widetilde{\mathcal{R}}_0$ to compare the contribution of different transmission mechanisms on the initial infection risk.

Additionally, we fit the model to the reported GBS surveillance data in northeastern region of Brazil and estimated the ratio of reported excess GBS cases to ZIKV cases. Both local and global sensitivity analysis on the basic reproduction number $\mathcal{R}_0$ were performed. We found that the vector-host interaction parameters, particularly the mosquito biting rate, ratio of mosquitoes to humans and mortality rate of mosquitoes, have a strong impact on $\mathcal{R}_0$, whereas $\mathcal{R}_0$ is much less sensitive to parameters related to sexual transmission in humans and vertical transmission in mosquitoes. A numerical example was given to demonstrate the sharp threshold dynamics of the model system. The endemic equilibrium when exists is a stable focus. The second example is devoted to quantitatively assess the relative contribution of every transmission mode. The mosquito-borne transmission makes the biggest contribution to both the reproduction number and the host infections, following by sexual transmission and vertical transmission. It is worthy pointing out that their relative contributions vary over time, and sexual transmission plays an important role in the early phase of a Zika outbreak. In other words, neglecting sexual transmission will underestimate the basic reproduction number and the size of human infections where the percentages of relative underestimation can be over 5% and up to 10%, respectively. From the perspective of disease control, taking precautions to prevent mosquito bites (via insect repellent, insecticide-treated net, etc.) is always a core measure in fight against Zika. However, the importance of avoiding unprotected sexual intercourse need to be addressed especially before the peak of the first epidemic wave. Although the relative contribution of vertical transmission to Zika fever is small, it may play an important role in maintaining the circulation of the virus in arid and semiarid areas—like the case of Rift Valley fever (Linthicum et al. 1999). Since infected *Aedes* eggs can survive dry conditions for long periods and hatch following the rainy season, a new wave of Zika infections could occur once the infected larvae mature.

We generalize the Bailey–Dietz model by incorporating sexual transmission in hosts and vertical transmission in vectors. Several existing studies assessed the relative role of sexual transmission on the basic reproduction number of Zika (Gao et al. 2016; Maxian et al. 2017; Towers et al. 2016). Recently, Olawoyin and Kribs (2018) proposed a complicated epidemic model with four transmission pathways. They did not do theoretical analysis due to model complexity but performed extensive numer-

ical simulations to reveal the effects of the secondary transmission routes of Zika on the basic reproduction number, the peak time and the final size. Differing from Olawoyin and Kribs (2018), our model structure enables us to do rigorous mathematical analysis. Moreover, they discussed the role of secondary transmission routes by comparing the models with and without secondary transmission routes, whereas our study was based on splitting the basic reproduction number and the host infection rate of a unique model into different parts corresponding to different routes. In particular, we quantitatively evaluated the relative contribution of each transmission mode on the basic reproduction number, the short- and long-term host infections. Based on a complicated epidemic model, Gao et al. (2016) estimated that the percentage of contribution by sexual transmission in the basic reproduction number is 3.044% (95% CI: 0.123–45.73). The fraction of basic reproduction number due to sexual transmission obtained by Towers et al. (2016) was 23% (95% CI: 1–47), while Maxian et al. (2017) and Olawoyin and Kribs (2018) estimated that sexual transmission contributes 5% or less to the reproduction number. In current study, we estimated that sexual transmission and vertical transmission contribute 1.4% and 0.2% to the basic reproduction number $\widetilde{\mathcal{R}}_0$, respectively, which are relatively small but still comparable with previous estimates. The sensitivity analysis reveals that $\mathcal{R}_0$ is most sensitive to mosquito biting rate, and insensitive to parameters involved in the secondary transmission pathways, which also agrees with existing works (Gao et al. 2016; Maxian et al. 2017; Olawoyin and Kribs 2018).

There is still much room for improvement. It is helpful to know how the relative contribution of each transmission mode changes with controllable model parameters. Since mosquitoes have a short lifespan, ignoring the extrinsic incubation period of the virus in mosquitoes could result in an overestimate of the infection risk. Further, we can include more epidemiological and biological factors like seasonal change in mosquito abundance (Gao et al. 2014), vertical transmission in humans (Besnard et al. 2014), human behavior change, life cycle of mosquitoes, antibody-dependent enhancement (Tang et al. 2019), spatial heterogeneity, alternative blood sources and so on.

Acknowledgements The authors thank the referees and the handling editor for valuable comments and suggestions that improved the original manuscript. This work was partially supported by the National Natural Science Foundation of China (12071300, 12071393 and 12071115), and the Natural Science Foundation of Shanghai (20ZR1440600 and 20JC1413800).

Appendix A: Proof of Theorem 3

Proof It follows from Theorem 2 that the global asymptotic stability of E_0 implies that there is no endemic equilibrium as $\mathcal{R}_0 \leq 1$. The above analysis indicates the existence and uniqueness of an endemic equilibrium as $\mathcal{R}_0 > 1$. It only remains to show the local asymptotic stability of $E^* = (I_h^*, R_h^*, I_v^*)$ whenever it exists. The equilibrium

equations (5) can be rewritten as

$$\begin{aligned}
&\left(\frac{ab}{H}I_v^* + \frac{\beta}{H}I_h^*\right)S_h^* = (\gamma + \mu_h)I_h^*,\\
&\gamma I_h^* = \mu_h R_h^*,\\
&\frac{ac}{H}I_h^* S_v^* = \mu_v(1-\theta)I_v^*,
\end{aligned} \tag{A.1}$$

where $S_h^* = H - I_h^* - R_h^*$ and $S_v^* = M - I_v^*$. It follows from the first equation of (A.1) that

$$\gamma + \mu_h > \frac{\beta}{H}S_h^*. \tag{A.2}$$

Multiplying both sides of the first and third equations of (A.1) gives

$$\left(\frac{ab}{H}I_v^* + \frac{\beta}{H}I_h^*\right)S_h^*\frac{ac}{H}I_h^* S_v^* = (\gamma + \mu_h)I_h^*\mu_v(1-\theta)I_v^*.$$

Thus,

$$\frac{ab}{H}\frac{ac}{H}S_h^* S_v^* = (\gamma + \mu_h)\mu_v(1-\theta) - \frac{\beta}{H}\frac{ac}{H}I_h^* S_h^*\frac{S_v^*}{I_v^*}. \tag{A.3}$$

The Jacobian matrix of system (2) at the endemic equilibrium E^* is

$$J(E^*) = \begin{pmatrix} J_{11} & -\frac{ab}{H}I_v^* - \frac{\beta}{H}I_h^* & \frac{ab}{H}(H - I_h^* - R_h^*)\\ \gamma & -\mu_h & 0\\ \frac{ac}{H}(M - I_v^*) & 0 & -\frac{ac}{H}I_h^* - \mu_v(1-\theta)\end{pmatrix},$$

where

$$J_{11} = -\frac{ab}{H}I_v^* - \frac{\beta}{H}I_h^* + \frac{\beta}{H}(H - I_h^* - R_h^*) - \gamma - \mu_h.$$

Using the first and third equations in (A.1), it can be rewritten as

$$J(E^*) = \begin{pmatrix} J_{11}^* & -\frac{ab}{H}I_v^* - \frac{\beta}{H}I_h^* & \frac{ab}{H}S_h^*\\ \gamma & -\mu_h & 0\\ \frac{ac}{H}S_v^* & 0 & -\mu_v(1-\theta)\left(1 + \frac{I_v^*}{S_v^*}\right)\end{pmatrix},$$

where $J_{11}^* = -(\gamma+\mu_h)\left(1+\frac{I_h^*}{S_h^*}\right)+\frac{\beta}{H}S_h^*$. The characteristic equation of $J(E^*)$ is given by

$$\begin{aligned} p(\lambda) =&(\lambda+\mu_h)(\lambda^2+b_1\lambda+b_0)\\ &+\gamma\left(\lambda+\mu_v(1-\theta)\left(1+\frac{I_v^*}{S_v^*}\right)\right)\left(\frac{ab}{H}I_v^*+\frac{\beta}{H}I_h^*\right)=0, \end{aligned}$$

where

$$\begin{aligned} b_1 =&(\gamma+\mu_h)\left(1+\frac{I_h^*}{S_h^*}\right)-\frac{\beta}{H}S_h^*+\mu_v(1-\theta)\left(1+\frac{I_v^*}{S_v^*}\right)\\ >&\gamma+\mu_h-\frac{\beta}{H}S_h^*+\mu_v(1-\theta)\left(1+\frac{I_v^*}{S_v^*}\right)\\ >&\mu_v(1-\theta)\left(1+\frac{I_v^*}{S_v^*}\right)>0, \end{aligned} \tag{A.4}$$

and

$$b_0=\left((\gamma+\mu_h)\left(1+\frac{I_h^*}{S_h^*}\right)-\frac{\beta}{H}S_h^*\right)\mu_v(1-\theta)\left(1+\frac{I_v^*}{S_v^*}\right)-\frac{ab}{H}\frac{ac}{H}S_h^*S_v^*.$$

Substituting (A.3) into the above expression gives

$$\begin{aligned} b_0 =&\left((\gamma+\mu_h)\left(1+\frac{I_h^*}{S_h^*}\right)-\frac{\beta}{H}S_h^*\right)\mu_v(1-\theta)\left(1+\frac{I_v^*}{S_v^*}\right)\\ &-\left((\gamma+\mu_h)\mu_v(1-\theta)-\frac{\beta}{H}\frac{ac}{H}I_h^*S_h^*\frac{S_v^*}{I_v^*}\right)\\ =&(\gamma+\mu_h)\mu_v(1-\theta)\left(\left(1+\frac{I_h^*}{S_h^*}\right)\left(1+\frac{I_v^*}{S_v^*}\right)-1\right)\\ &+\frac{\beta}{H}S_h^*\left(\frac{ac}{H}I_h^*\frac{S_v^*}{I_v^*}-\mu_v(1-\theta)\left(1+\frac{I_v^*}{S_v^*}\right)\right), \end{aligned}$$

then, applying the third equation of (A.1) yields

$$b_0=(\gamma+\mu_h)\mu_v(1-\theta)\left(\left(1+\frac{I_h^*}{S_h^*}\right)\left(1+\frac{I_v^*}{S_v^*}\right)-1\right)-\frac{\beta}{H}S_h^*\mu_v(1-\theta)\frac{I_v^*}{S_v^*}.$$

Using the inequality (A.2), we obtain

$$\begin{aligned} b_0 >&(\gamma+\mu_h)\mu_v(1-\theta)\left(\left(1+\frac{I_h^*}{S_h^*}\right)\left(1+\frac{I_v^*}{S_v^*}\right)-1\right)-(\gamma+\mu_h)\mu_v(1-\theta)\frac{I_v^*}{S_v^*}\\ =&(\gamma+\mu_h)(1-\theta)\mu_v\left(\frac{I_h^*}{S_h^*}+\frac{I_h^*I_v^*}{S_h^*S_v^*}\right)>0. \end{aligned}$$

Expanding the characteristic polynomial $p(\lambda)$ yields

$$p(\lambda) = \lambda^3 + B_2\lambda^2 + B_1\lambda + B_0 = 0,$$

where

$$\begin{aligned}
B_2 &= b_1 + \mu_h > 0,\\
B_1 &= b_0 + b_1\mu_h + \gamma\left(\frac{ab}{H}I_v^* + \frac{\beta}{H}I_h^*\right),\\
B_0 &= b_0\mu_h + \gamma\mu_v(1-\theta)\left(1 + \frac{I_v^*}{S_v^*}\right)\left(\frac{ab}{H}I_v^* + \frac{\beta}{H}I_h^*\right) > 0.
\end{aligned}$$

Direct calculation finds

$$\begin{aligned}
B_1B_2 - B_0 =&(b_1 + \mu_h)\left(b_0 + b_1\mu_h + \gamma\left(\frac{ab}{H}I_v^* + \frac{\beta}{H}I_h^*\right)\right)\\
&- b_0\mu_h - \gamma\mu_v(1-\theta)\left(1 + \frac{I_v^*}{S_v^*}\right)\left(\frac{ab}{H}I_v^* + \frac{\beta}{H}I_h^*\right)\\
>&b_1\gamma\left(\frac{ab}{H}I_v^* + \frac{\beta}{H}I_h^*\right) - \gamma\mu_v(1-\theta)\left(1 + \frac{I_v^*}{S_v^*}\right)\left(\frac{ab}{H}I_v^* + \frac{\beta}{H}I_h^*\right)\\
=&\gamma\left(\frac{ab}{H}I_v^* + \frac{\beta}{H}I_h^*\right)\left(b_1 - \mu_v(1-\theta)\left(1 + \frac{I_v^*}{S_v^*}\right)\right).
\end{aligned}$$

By using inequality (A.4), we finally get

$$B_1B_2 - B_0 > 0.$$

Following the Routh–Hurwitz criterion, all eigenvalues of $J(E^*)$ have negative real parts. Therefore, the endemic equilibrium E^* of system (2) is locally asymptotically stable. □

References

Agusto FB, Bewick S, Fagan WF (2017a) Mathematical model for Zika virus dynamics with sexual transmission route. Ecol Complex 29:61–81

Agusto FB, Bewick S, Fagan WF (2017b) Mathematical model of Zika virus with vertical transmission. Infect Dis Model 2(2):244–267

Andraud M, Hens N, Marais C, Beutels P (2012) Dynamic epidemiological models for dengue transmission: a systematic review of structural approaches. PLoS ONE 7(11):e49085

Arriola L, Hyman JM (2009) Sensitivity analysis for uncertainty quantification in mathematical models. In: Chowell G, Hyman JM, Bettencourt LMA, Castillo-Chavez C (eds) Mathematical and statistical estimation approaches in epidemiology. Springer, New York, pp 195–247

Baca-Carrasco D, Velasco-Hernández JX (2016) Sex, mosquitoes and epidemics: an evaluation of Zika disease dynamics. Bull Math Biol 78(11):2228–2242

Bates S, Hutson H, Rebaza J (2021) Global stability of Zika virus dynamics. Differ Equ Dyn Syst 29(3):657–672

Besnard M, Lastère S, Teissier A, Cao-Lormeau VM, Musso D (2014) Evidence of perinatal transmission of Zika virus. French Polynesia, December 2013 and February 2014. Euro Surveill 19(13):pii=20751
Brady OJ, Osgood-Zimmerman A, Kassebaum NJ et al (2019) The association between Zika virus infection and microcephaly in Brazil 2015–2017: an observational analysis of over 4 million births. PLoS Med 16(3):e1002755
Brauer F, Castillo-Chavez C, Feng Z (2019) Mathematical models in epidemiology. Springer, New York
Brauer F, Castillo-Chavez C, Mubayi A, Towers S (2016) Some models for epidemics of vector-transmitted diseases. Infect Dis Model 1(1):79–87
Chikaki E, Ishikawa H (2009) A dengue transmission model in Thailand considering sequential infections with all four serotypes. J Infect Dev Countries 3(9):711–722
Dallas County Health and Human Services (DCHHS) (2016) DCHHS Reports first Zika virus case in Dallas County acquired through sexual transmission. https://www.dallascounty.org/department/hhs/documents/DCHHS_Zika. Accessed on 10 April 2021
de Araújo TVB, Ximenes RAA, Miranda-Filho DB et al (2018) Association between microcephaly, Zika virus infection, and other risk factors in Brazil: final report of a case-control study. Lancet Infect Dis 18:328–336
de Castro Medeiros LC, Castilho CAR, Braga C, de Souza WV, Regis L, Monteiro AMV (2011) Modeling the dynamic transmission of dengue fever: investigating disease persistence. PLoS Negl Trop Dis 5(1):e942
de Oliveira WK, Carmo EH, Henriques CM et al (2017) Zika virus infection and associated neurologic disorders in Brazil. N Engl J Med 376(16):1591–1593
Dick GWA, Kitchen SF, Haddow AJ (1952) Zika virus. I. Isolations and serological specificity. Trans R Soc Trop Med Hyg 46(5):509–520
Diekmann O, Heesterbeek JAP, Metz JAJ (1990) On the definition and the computation of the basic reproduction ratio R_0 in models for infectious diseases in heterogeneous populations. J Math Biol 28(4):365–382
Duffy MR, Chen T, Hancock WT et al (2009) Zika virus outbreak on Yap Island, Federated States of Micronesia. N Engl J Med 360:2536–2543
Foy BD, Kobylinski KC, Foy JLC, Blitvich BJ, Travassos da Rosa A, Haddow AD, Lanciotti RS, Tesh RB (2011) Probable non-vector-borne transmission of Zika virus, Colorado, USA. Emerg Infect Dis 17(5):880–882
Gao D, Lou Y, He D, Porco TC, Kuang Y, Chowell G, Ruan S (2016) Prevention and control of Zika as a mosquito-borne and sexually transmitted disease: a mathematical modeling analysis. Sci Rep 6:28070
Gao D, Lou Y, Ruan S (2014) A periodic Ross–Macdonald model in a patchy environment. Discrete Contin Dyn Syst Ser B 19(10):3133–3145
He D, Ionides EL, King AA (2010) Plug-and-play inference for disease dynamics: measles in large and small populations as a case study. J R Soc Interface 7(43):271–283
He D, Zhao S, Lin Q, Musa SS, Stone L (2020) New estimates of the Zika virus epidemic attack rate in Northeastern Brazil from 2015 to 2016: a modelling analysis based on Guillain-Barré Syndrome (GBS) surveillance data. PLoS Neg Trop Dis 14(4):e0007502
Heukelbach J, Alencar CH, Kelvin AA, de Oliveira WK, de Góes Cavalcanti LP (2016) Zika virus outbreak in Brazil. J Infect Dev Ctries 10(2):116–120
Imran M, Usman M, Dur-e-Ahmad M, Khan A (2021) Transmission dynamics of Zika fever: a SEIR based model. Differ Equ Dyn Syst 29:463–486
Kucharski AJ, Funk S, Eggo RM, Mallet HP, Edmunds WJ, Nilles EJ (2016) Transmission dynamics of Zika virus in island populations: a modelling analysis of the 2013–14 French Polynesia outbreak. PLoS Neg Trop Dis 10(5):e0004726
Lai Z, Zhou T, Zhou J, Liu S, Xu Y, Gu J, Yan G, Chen X (2020) Vertical transmission of Zika virus in Aedes albopictus. PLoS Negl Trop Dis 14(10):e0008776
Lasalle JP (1976) The stability of dynamical systems. SIAM, Philadephia
Linthicum KJ, Anyamba A, Tucker CJ, Kelley PW, Myers MF, Peters CJ (1999) Climate and satellite indicators to forecast Rift Valley fever epidemics in Kenya. Science 285:397–400
MacNamara FN (1954) Zika virus: a report on three cases of human infection during an epidemic of jaundice in Nigeria. Trans R Soc Trop Med Hyg 48(2):139–145
Manore CA, Hickmann KS, Xu S, Wearing HJ, Hyman JM (2014) Comparing dengue and chikungunya emergence and endemic transmission in *A. aegypti* and *A. albopictus*. J Theor Biol 356:174–191

Marino S, Hogue IB, Ray CJ, Kirschner DE (2008) A methodology for performing global uncertainty and sensitivity analysis in systems biology. J Theor Biol 254:178–196
Maxian O, Neufeld A, Talis EJ, Childs LM, Blackwood JC (2017) Zika virus dynamics: when does sexual transmission matter? Epidemics 21:48–55
Mier-y-Teran-Romero L, Delorey MJ, Sejvar JJ, Johansson MA (2018) Guillain–Barré syndrome risk among individuals infected with Zika virus: a multi-country assessment. BMC Med 16:67
Mlakar J, Korva M, Tul N et al (2016) Zika virus associated with microcephaly. N Engl J Med 374(10):951–958
Moreira J, Peixoto TM, Siqueira AM, Lamas CC (2017) Sexually acquired Zika virus: a systematic review. Clin Microbiol Infect 23(5):296–305
Musso D, Nilles EJ, Cao-Lormeau V-M (2014) Rapid spread of emerging Zika virus in the Pacific area. Clin Microbiol Infect 20(10):595–596
Olawoyin O, Kribs C (2018) Effects of multiple transmission pathways on Zika dynamics. Infect Dis Model 3:331–344
Pan American Health Organization (2016) Neurological syndrome, congenital malformations and Zika virus infection
Parra B, Lizarazo J, Jiménez-Arango JA et al (2016) Guillain–Barré Syndrome associated with Zika virus infection in Colombia. N Engl J Med 375(16):1513–1523
Polen KD, Gilboa SM, Hills S et al (2018) Update: Interim guidance for preconception counseling and prevention of sexual transmission of Zika virus for men with possible Zika virus exposure-United States. MMWR Morb Mortal Wkly Rep 67(31):868–871
Rasmussen SA, Jamieson DJ, Honein MA, Petersen LR (2016) Zika virus and birth defects-reviewing the evidence for causality. N Engl J Med 374(20):1981–1987
Roser M, Ortiz-Ospina E, Ritchie H (2019) Life Expectancy. https://ourworldindata.org/life-expectancy. Accessed on 10 April 2021
Saad-Roy CM, Ma J, van den Driessche P (2018) The effect of sexual transmission on Zika virus dynamics. J Math Biol 77(6–7):1917–1941
Sariol CA, Nogueira ML, Vasilakis N (2018) A tale of two viruses: does heterologous flavivirus immunity enhance Zika disease? Trends Microbiol 26(3):186–190
Shutt DP, Manore CA, Pankavich S, Porter AT, Del Valle SY (2017) Estimating the reproductive number, total outbreak size, and reporting rates for Zika epidemics in South and Central America. Epidemics 21:63–79
Souza MO (2014) Multiscale analysis for a vector-borne epidemic model. J Math Biol 68(5):1269–1293
Tang B, Zhou W, Xiao Y, Wu J (2019) Implication of sexual transmission of Zika on dengue and Zika outbreaks. Math Biosci Eng 16(5):5092–5113
Thangamani S, Huang J, Hart CE, Guzman H, Tesh RB (2016) Vertical transmission of Zika virus in Aedes aegypti mosquitoes. Am J Trop Med Hyg 95(5):1169–1173
Thieme HR (1993) Persistence under relaxed point-dissipativity (with application to an endemic model). SIAM J Math Anal 24(2):407–435
Towers S, Brauer F, Castillo-Chavez C, Falconar AKI, Mubayi A, Romero-Vivas CME (2016) Estimate of the reproduction number of the 2015 Zika virus outbreak in Barranquilla, Colombia, and estimation of the relative role of sexual transmission. Epidemics 17:50–55
van den Driessche P, Watmough J (2002) Reproduction numbers and sub-threshold endemic equilibria for compartmental models of disease transmission. Math Biosci 180:29–48
Wang L, Zhao H, Oliva SM, Zhu H (2017) Modeling the transmission and control of Zika in Brazil. Sci Rep 7(1):7721
Wiratsudakul A, Suparit P, Modchang C (2018) Dynamics of Zika virus outbreaks: an overview of mathematical modeling approaches. PeerJ 6:e4526
World Health Organization (2016) WHO statement on the first meeting of the International Health Regulations (2005) (IHR 2005) Emergency Committee on Zika virus and observed increase in neurological disorders and neonatal malformations,https://www.who.int/news/item/01-02-2016-who-statement-on-the-first-meeting-of-the-international-health-regulations-(2005)-(ihr-2005)-emergency-committee-on-zika-virus-and-observed-increase-in-neurological-disorders-and-neonatal-malformations. Accessed on 10 April 2021
World Health Organization (2016) The History of Zika Virus, https://www.who.int/news-room/feature-stories/detail/the-history-of-zika-virus. Accessed on 10 April 2021

World Health Organization (2017) Zika Situation Report. https://www.who.int/emergencies/zika-virus/situation-report/10-march-2017/en/. Accessed on 10 March 2017
World Health Organization. Zika Virus Disease. https://www.who.int/health-topics/zika-virus-disease. Accessed on 10 April 2021